Available online at www.sciencedirect.com
SCIENCE DIRECT®
International Journal of Fatigue 25 (2003) 1389–1398
International Journal of Fatigue
www.elsevier.com/locate/ijfatigue

Weld tool travel speed effects on fatigue life of friction stir welds in 5083 aluminium

M.N. James [a,*], D.G. Hattingh [b], G.R. Bradley [a]

[a] Department of Mechanical & Marine Engineering, University of Plymouth, Drake Circus, Plymouth PL4 8AA, Devon, UK
[b] Mechanical Engineering, PE Technikon, Private Bag X6011 Port Elizabeth, South Africa

Received 15 July 2002; received in revised form 13 December 2002; accepted 7 January 2003

Abstract

This paper reports the results of a study into the influence of weld tool travel speed (in the range 80–200 mm/min) on the occurrence of 'onion-skin' forging-type defects (similar to the root defects known as 'kissing bonds') in single pass friction stir (SP FS) welds, and on the effect of these defects on fatigue crack initiation and overall life. Results indicate that such defects are generally not associated with fatigue crack initiation, but may act to reduce fatigue life by providing easy linking paths between two fatigue cracks. It is likely that their influence on fracture toughness of SP FS welds would be higher, as they occur more readily when growth rates and levels of plastic deformation are higher.

1. Introduction

Friction stir welding (FSW) is a relatively new solid-state joining technique, which offers high joint quality and good fatigue performance. Other advantages include little, or no, joint preparation, relatively few defects and little requirement for post-weld dressing. In FSW, a cylindrical, shouldered tool with a profiled probe, or pin (slightly smaller in length than the plate thickness), is rotated (typically at around 500 rpm) and slowly plunged into the joint line between two abutting pieces of plate or sheet that are to be joined. The parts must be clamped to prevent the joint faces being forced apart. Adiabatic shear and friction generate heat between the wear resistant tool and the plate. The material softens and flows around the tool as it is progressed along the joint line. Forging occurs under the pressure applied by the tool shoulder, which is inclined at a slight angle (around 2.5°) to the horizontal. The process approximates a solid-state keyhole welding process, in that a hole to accommodate the pin is generated, then filled as the weld is made.

The recrystallisation of the microstructure that occurs under the high levels of plastic strain induced in the weld, leads to a very fine-grained structure in the weld nugget, as shown in Fig. 1 for the 5383-H321 alloy. Typical FSW terminology is also indicated in the figure. It is useful to distinguish between advancing and retreating sides (advancing representing the side in which rotational direction and weld travel direction are additive) because of differing residual stresses and strains at these locations [1], which influences crack initiation and crack growth [2]. It is usual to refer to thermo-mechanically affected zones (TMAZs) in FSW, as well as heat-affected zones (HAZs).

As stated before, defect levels are generally low in FSW, compared with typical fusion welds. A number of types of defect are known to occur, however, and because they can occur in any orientation and at any angle, may be difficult to detect with directionally specific techniques such as radiography and ultrasonics [3]. The known defects in FS butt welds include lack of penetration (tool length too small for the plate thickness), voids and root defects, which are also known as 'kissing bonds'. These occur when the root of a single pass (SP) weld achieves only partial bonding and some influences of their effect on fatigue strength are covered in another article in this issue of the journal [4]. The occurrence of kissing bonds appears to be alloy specific and in particular, in the limited range of alloys considered, 5038-

* Corresponding author. Tel.: +44-1752-233300; fax: +44-1752-233310.
E-mail address: neil.james@plymouth.ac.uk (M.N. James).

0142-1123/$ - see front matter © 2003 Elsevier Ltd. All rights reserved.
doi:10.1016/S0142-1123(03)00061-6

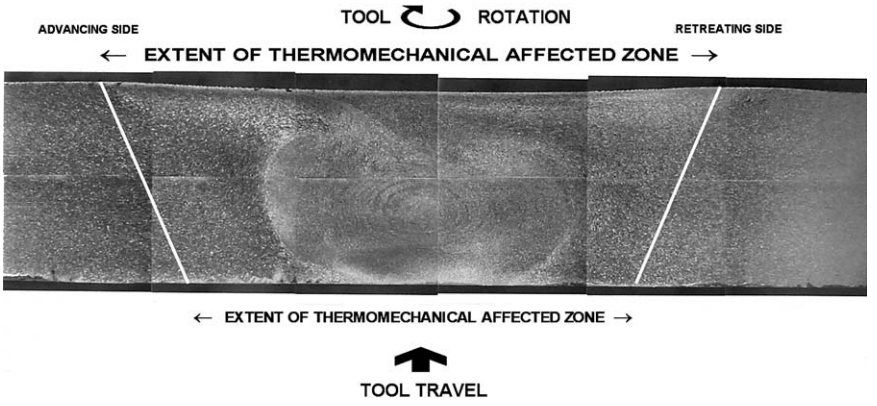

Fig. 1. Macrograph of a SP friction stir weld in 8 mm 5383-H321 aluminium plate (5383 alloy is very similar in composition and weld characteristics to 5083).

H321 is known to be more susceptible to these defects than either 5083-O or 6082-T6 alloys [4]. The relative difficulty of detecting defects in FS welds makes it imperative to fully understand the influence of any defects on fatigue crack initiation and total life. As yet, however, there are few reported studies on the fatigue performance of FS welds in the open literature, and those that are reported are often preliminary in nature [5]. Thus, there is an absence of detailed information, particularly regarding internal defects, their origin and their influence on fatigue crack initiation and life.

Work in our laboratory on 5383-H321 and 5083-H321 aluminium alloys using SP and double pass (DP) welds, has indicated that occasional defect-like features do occur on the fracture surfaces of fatigue specimens. They may occur in groups, reminiscent of the 'onion-skin' rings in the weld nugget, may be up to several millimetres in length, and occur particularly in the case of SP welds. The fact that defects occur internally, apparently associated with artefacts of the plastic flow, is perhaps unsurprising considering the chaotic nature of the plastic deformation in the weld nugget [6]. Bendzsak et al. [6] in their paper on 3D modelling of FS welding, state that the chaotic flow region formed below the tool shoulder, on the advancing side of the weld, contains flow singularities. These singularity regions in a weld correspond with defect locations and are likely to be affected by tool rotational speed, travel speed during welding and geometry of the tool [6].

It is therefore expected that tool travel and rotational speeds would be prime parameters governing the occurrence of internal defects in FS welds. As these parameters are usually determined from empirical knowledge and trial runs on test plates, it would be advantageous to know the effect of variations in these parameters on the defect population and fatigue life. The effect of these parameters on fatigue life has been considered in another article in this issue of the journal [7], which studied FS welds in 4 mm plate of 6082-T6 and 6082-T4 aluminium alloys, and concluded that it had no major effect in that alloy. That study used tool travel speeds of 700 and 1400 mm/min, and rotation speeds of 2200 and 2500 rpm, respectively. Inspection of their *S–N* data, however, indicates that an effect of weld speed on slope of the data is present, and that the data sets are too small to draw statistically meaningful conclusions.

The present paper reports the results of a study of the effect of tool travel speed on defect formation in 8 mm thick plates of 5083-H321 aluminium alloy, and their influence on fatigue crack initiation and life. Values of tool rotational and travel speeds used in the present study are significantly lower than those pertaining to the work of Ericsson and Sandström [7], the results obtained indicate a definite effect of travel speed on fatigue life.

In future work, it would be desirable to perform a more complete study of the influences of tool design, rotational and travel speeds on internal FSW defects. The initial work performed on SP FS welds had observed internal defects in specimens that had been subjected to four-point bending fatigue. The defects were not associated with crack initiation, but generally occurred towards the centre of the specimens, often in the region of fast fracture (Fig. 2). The origin of these defect-like features was not clear, but their appearance was usually consistent with partial forging along onion-skin layers in the weld nugget (Fig. 2(a)). Some defects could arise also from a fluid dynamics voiding effect (Fig. 2(b)), either associated with the singularities mentioned before, or possibly due to vortex generation behind the tool probe as it makes the weld.

The remit of this work was therefore to examine the effect of weld travel speed on the frequency of occurrence of internal FS weld defects, for a single tool rotation speed. The objective was to ascertain the influence of the defects on fatigue crack initiation and life in 5083-H321 aluminium alloy, which was known to be relatively susceptible to kissing bonds [4]. A secondary objective was to determine whether the defects became more like voids as tool travel speed increased. This was intended to shed some light on their origin, as being

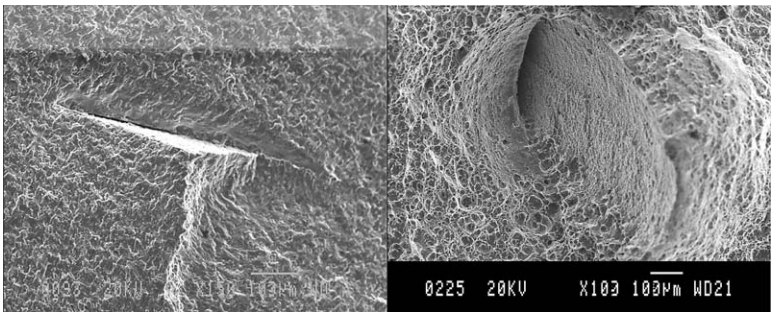

Fig. 2. Fractographs of SP FSW fracture surfaces. (a) Left side: apparent defect on fatigue region; (b) right side: apparent defect/void in fast fracture region.

either vortex shedding or singularity induced. In this work specimens were loaded in tension, rather than bend, so as to uniformly stress the complete specimen cross-section, and hence be more likely to activate incipient defects as crack initiation sites.

2. Material and experimental conditions

Plates of rolled 5083-H321 aluminium alloy, 8 mm thick, 1000 mm long and 500 mm wide were used in this investigation. Two such plates were welded together to form the stock from which fatigue specimens were machined. Parent plate properties are given in Table 1, where $\sigma_{0.2\%}$ is the 0.2% proof strength and σ_{TS} is the tensile strength. Alloy 5083 is a weldable, strain hardening structural alloy suitable for marine applications, and 8 mm is the common thickness used in shipbuilding. The H321 designation represents a strain hardened and stabilised condition, with the alloy approximating the quarter-hard state after the thermal stabilisation treatment.

FSW (either SP or DP) reduces the 0.2% proof strength in the weld region to around 160 MPa. Vickers hardness values under a 200 gf load drop from around 105 in the parent plate to 81–85 within the TMAZ, which extends out to about 15 mm either side of the weld centre-line. These hardness values are little affected by travel speed, as indicated in Fig. 3 for a very similar 5383-H321 plate welded at 80 mm/min and for 5083-H321 welded at 200 mm/min. The mean hardness value in the weld metal with the faster travel speed is perhaps 90 Vickers, while that for the 80 mm/min travel speed is around 87.5 Vickers.

Table 1
Parent plate properties of 5083-H321 aluminium alloy

Weight %	Mg	Mn	Si	Fe	Cr	Zn	Cu	Ti	$\sigma_{0.2\%}$ (MPa)	σ_{TS} (MPa)
5083-H321	4.20	0.60	0.25	0.15	0.09	0.09	0.06	0.02	264	350

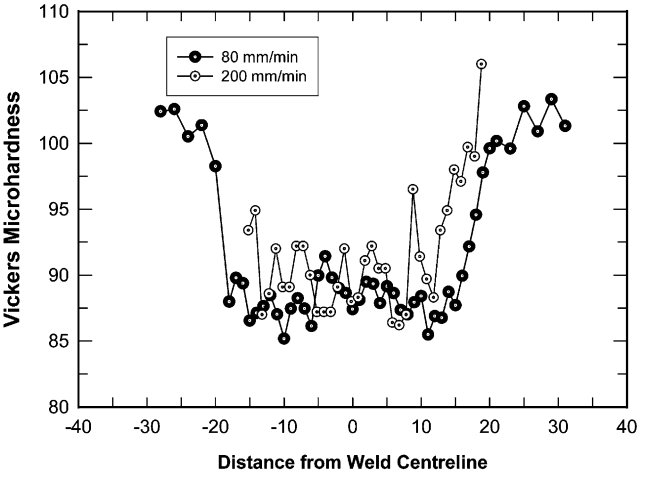

Fig. 3. Typical microhardness data for single pass (SP) and double pass (DP) welds in 5383-H321 aluminium alloy for 80 and 200 mm/min tool travel speeds.

The SP welds were made at TWI, Abington, with a Type 5651 tool, which had a 25 mm shoulder, and a 10 mm diameter pin of length 7.9 mm. Tool rotation was kept constant at 500 rpm clockwise, looking at the plate, with a forwards tilt in the direction of travel of 2.5° and a heel plunge depth of 0.2 mm. Weld travel speed in the bend testing had originally been 70 mm/min, and the four higher travel speeds used in this work were 80, 95, 130 and 200 mm/min.

Rectangular section, hourglass shaped fatigue specimens were machined from the plates. Gauge length of the specimens was 40 mm, width 16 mm and thickness was kept as close as possible to the original plate size of approximately 8 mm. A 100 mm radius was used to connect the gauge length to the grip sections, and the edges were slightly rounded to prevent crack initiation occurring there. *S–N* testing was performed in tension at 112 Hz and R = −1 (fully reversed loading). Two specimen surface conditions were used; as-welded, with small burrs at the edges of the weld region removed, but the tool shoulder ledges (~0.2 mm) remaining, and machined, where both burrs and ledges had been removed, leaving a smooth surface free of stress concen-

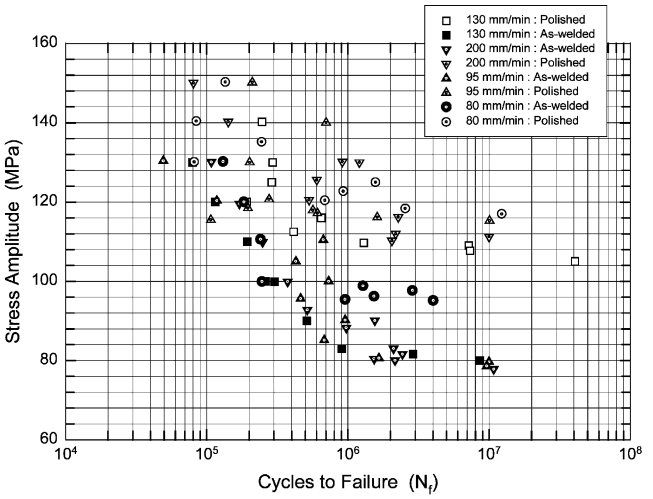

Fig. 4. Tensile fatigue (*S–N*) data at R = −1 for SP FSW in 5083-H321 aluminium alloy. Four travel speeds (in the range 80–200 mm/min), and two surface conditions (as-welded and polished) were considered.

trations (net thickness about 7.4 mm). This was done because there was an interest in both the fatigue performance of as-welded samples, representing general engineering usage, and in the inherent fatigue properties of the welds as a function of travel speed, unaffected by surface artefacts induced by the welding process.

3. Fatigue (*S–N*) data

Figs. 4 and 5 show the *S–N* results obtained, while Figs. 6 and 7 provide representative macrographs of the fracture surfaces of as-welded and polished specimens for all four tool travel speeds, respectively. For the as-welded specimens, crack initiation is always associated with surface tool rotation marks, while for the case of polished specimens crack initiation reflects either slip band cracking or small internal voids.

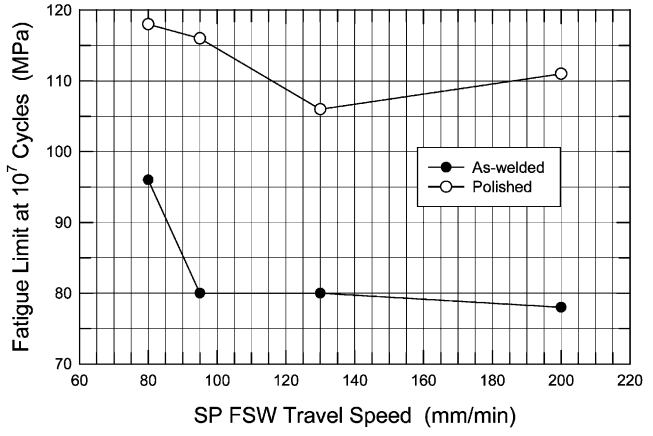

Fig. 5. Plot of fatigue limit corresponding to life of 10^7 cycles, as a function of SP FSW travel speed.

The real area of interest to structures is the long life regime ($N_f > 10^6$ cycles), particularly as aluminium alloys do not generally show a fatigue limit asymptote. Data were therefore obtained for $N_f \sim 10^7$ cycles in all cases, except for the 80 mm/min travel speed as-welded case, where the curve had apparently, become virtually asymptotic to the *x*-axis at around 10^6 cycles. This is presumably due to initiation becoming controlled by surface notches at stresses around 96 MPa. The FSW process leaves circular arcs on the surface due to tool rotation and translation, which generally act as crack initiation sites in as-welded SP specimens (Fig. 8). Slopes in the long life region of the *S–N* curves vary, but are generally relatively low. Table 2 below gives a summary of the endurance limits at 10^7 cycles, and Fig. 5 shows the information graphically. Note the tests were run until fast fracture occurred, i.e. until cracks reached a critical size at each stress value.

It is clear that the as-welded specimens have lower endurance limit stress amplitudes at R = −1, than the polished specimens. Interestingly, the ranking also changes between the two conditions at 130 mm/min, although insufficient data are available to be certain that this reflects a real effect. The as-welded condition apparently represents a reduction in endurance limit stress (corresponding to a life of 10^7 cycles), relative to the polished condition, of some 19% at 80 m/min, 31% at 95 mm/min, 25% at 130 mm/min and 30% at 200 mm/min. Generally, a decrease in endurance limit stress (at 10^7 cycles) is observed in both as-welded and polished specimens, as travel speed increases from 80 to 200 mm/min. The decrease has a maximum value of about 11% for polished and 19% for as-welded specimens. This is a significant reduction in fatigue strength, and it would seem that the lowest speed does provide the best performance in terms of both absolute endurance limit value, and in terms of the smallest reduction in strength between the as-welded and polished conditions. It should, however, be borne in mind that the surface condition may also vary between specimens and could also be contributing to scatter.

It is worth giving some consideration to the effects on fatigue life of the weld-induced residual stresses, as level of residual stress will affect the mean stress during fatigue and hence the observed life. The general observation is that sustainable fatigue stress amplitude reduces for a given life as the level of mean stress increases (in accord with Goodman diagram concepts). Residual stresses have been measured in larger SP FSW specimens manufactured from the same 8 mm thick aluminium alloy plates (rectangular specimens some 150 mm along the weld and 190 mm transverse to the weld). These measurements have been made on plates welded with an 80 mm/min travel speed, using synchrotron radiation at the European Synchrotron Radiation Facility at

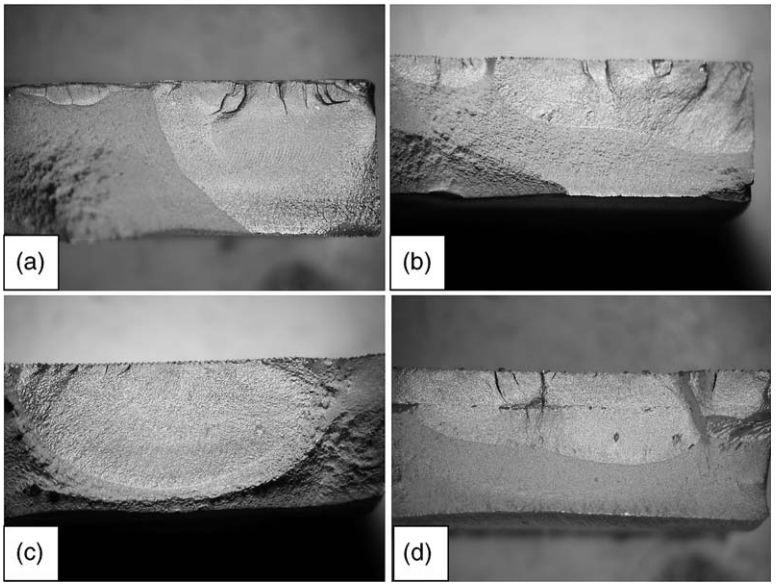

Fig. 6. Representative macrographs of the fracture surfaces of as-welded specimens: (a) 80, (b) 95, (c) 130, (d) 200 mm/min. Crack initiation sites are always on the upper surface in the pictures.

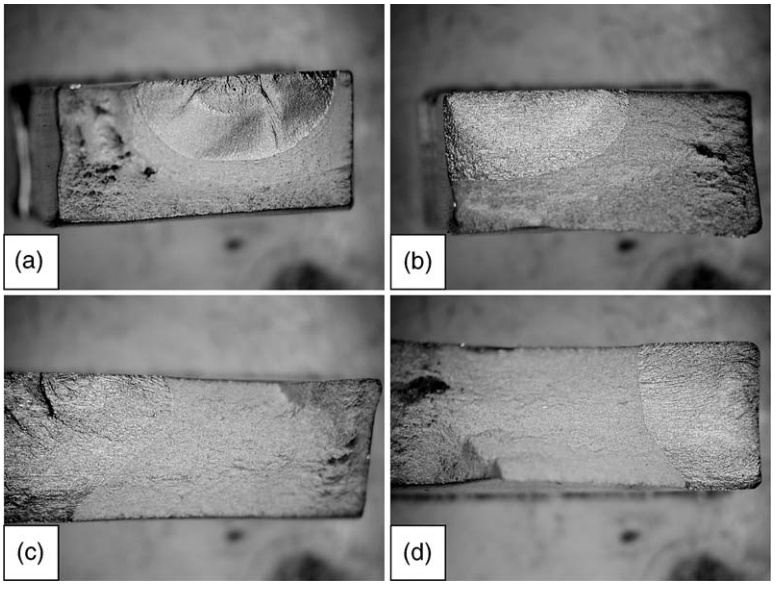

Fig. 7. Representative macrographs of the fracture surfaces of polished specimens: (a) 80, (b) 95, (c) 130, (d) 200 mm/min. Crack initiation sites are on the upper surface for (a)–(c), and at the right edge of the specimen in (d).

Grenoble, both in the as-welded state and after applying certain specific fatigue cycles.

These measurements indicate the possibility of significant variation, particularly in the peak compressive stresses, between different welded plates made under nominally identical welding conditions at a travel speed of 80 mm/min. Peak values of tensile stress in the as-welded state are relatively low at around 20–40 MPa, for both transverse and longitudinal directions in the plates, and these values occur some 16–18 mm from the weld centre-line. In the middle of the weld there is generally a slight dip observed in the value of tensile stress. Such low values of tensile stress, relative to the proof stress, reflect the low peak temperatures attendant on the FSW process.

In considering the effect of the residual stresses on the mean stress during fatigue cycling, the following points appear relevant.

- Peak tensile stress values are low for the 80 mm/min case and heat input per unit length would be lower with the higher travel speeds, giving an anticipated reduction in value of tensile residual stress.

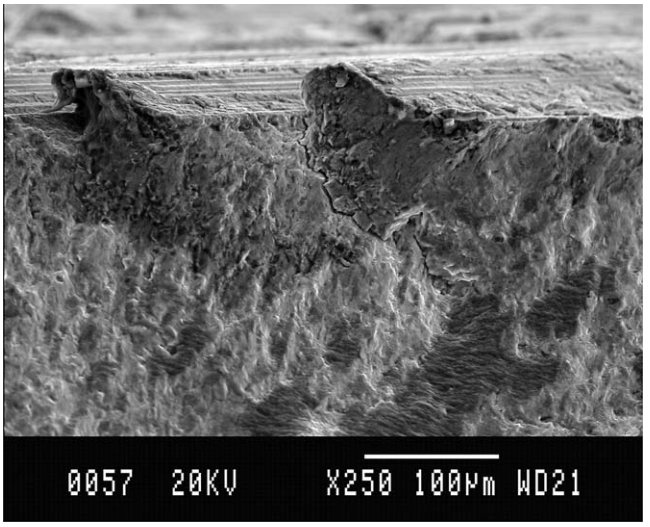

Fig. 8. Surface notches in SP welds arise from the combination of tool rotation and translation, and are often associated with crack initiation.

Table 2
Endurance limit stress amplitudes at 10^7 cycles for SP FSW specimens

Endurance limit (MPa)	Travel speed (mm/min)			
	80	95	130	200
Polished	118	116	106	111
As-welded	96	80	80	78
Reduction (%)	19	31	25	30

- These positions of peak tensile stress do not correspond very often with observed crack initiation sites.
- The much smaller weld length used in the *S–N* specimens (16 mm) compared with the plates used in residual stress measurements (150 mm) again indicates that lower residual stresses pertain to the *S–N* specimens.

The anticipated effect of residual stress on the *S–N* is therefore small, and it is the author's belief that the data represent largely intrinsic microstructural, and defect effects on fatigue life (hardness variation with travel speed appears to be a second order effect, as noted before). Equally, any residual stress effect should act to increase the observed decrease in fatigue strength concomitant with increase in tool travel speed.

From these data, it would initially seem that higher FSW travel speeds are more detrimental to fatigue strength at long lives, and one would therefore anticipate seeing more evidence of the defect-like features on the fracture surface, and of their involvement in crack initiation. However, as will be reported in the Section 4, this was not the case generally to be observed. The observed reduction in fatigue strength with travel speed generally reflects more subtle influences of defects and weld nugget texture.

These results are somewhat in contrast to those reported by Ericsson and Sandström [7] in their study on 6082 alloys. Two factors need to considered in this respect, first the known influence of alloy type on defect occurrence during FSW [4] and, secondly, the difference in range of fatigue data in the two studies. Ericsson and Sandström [7] run tests out to approximately 2×10^6 cycles, while the present study considers lives out to 10^7 cycles. Longer fatigue lives would tend to amplify any differences in fatigue strength arising from welding speed variation. Ericsson and Sandström [7] do, however, acknowledge an effect of welding speed on change in slope in their data, which varies between the T6 and T4 tempers of their alloy. Unfortunately, the magnitude of this effect is not quantified.

4. Fractography

Examination of the fracture surfaces at low magnification, using stereo-binoculars, did not indicate that defects were playing any greater role in crack initiation in these tensile specimens than previously observed for the case of the bend specimens. Fracture surface features, consistent with incomplete forging along onion-skin layers, were observed in a number of specimens, but were almost never associated with fatigue crack initiation. They tended to occur either towards the end of the fatigue region or, more frequently, in fast fracture areas. For specimens, which exhibited similar lives, but failed at higher and lower stresses, the principal cause of lower fatigue strength (at a given life) was observed to be multiple crack initiation. This was occasionally exacerbated when two fatigue cracks linked up by failure along onion-skin defects, i.e. along pseudo-lack-of-fusion type defects, similar to the kissing bonds observed at the root of FS welds [4]. Other cases involved voids in the crack initiation region.

These aspects can be illustrated using specific specimens. For example, data for two 200 mm/min as-welded specimens are D20: N_f = 1,533,900 at $\sigma_{amplitude}$ = 80.4 MPa and D10: N_f = 1,551,600 at $\sigma_{amplitude}$ = 90.1 MPa. D10 shows initiation from surface ridges (tool rotation artefacts), with onion-skin forging defects apparent towards the centre of the specimen both at the end of the fatigue region, and also more substantially in the fast fracture region (Fig. 9(a)). D20 also shows initiation from surface ridges and onion-skin forging defects occur only in the fast fracture region (Fig. 9(b)). Fig. 10 shows scanning electron micrographs (SEMs) of these onion-skin defects. The partial-forging defect in specimen D20 (Fig. 10(a)) had started to influence fracture in the fatigue region, and became fully developed

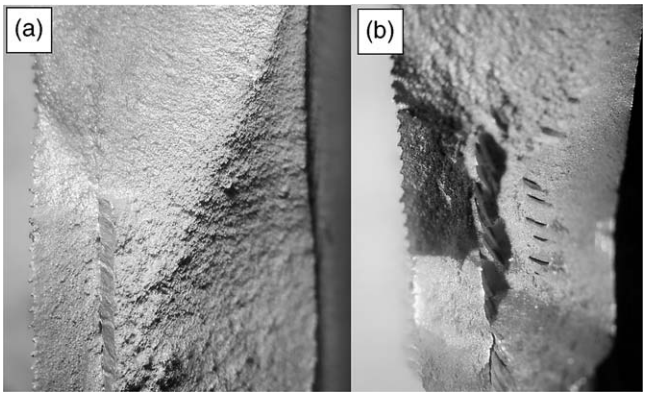

Fig. 9. Macroscopic fractographs showing two specimens welded at 200 mm/min: (a) Left—specimen D10: N_f = 1,533,900 at $\sigma_{amplitude}$ = 80.4 MPa; (b) right—specimen D20: N_f = 1,551,600 at $\sigma_{amplitude}$ = 90.1 MPa.

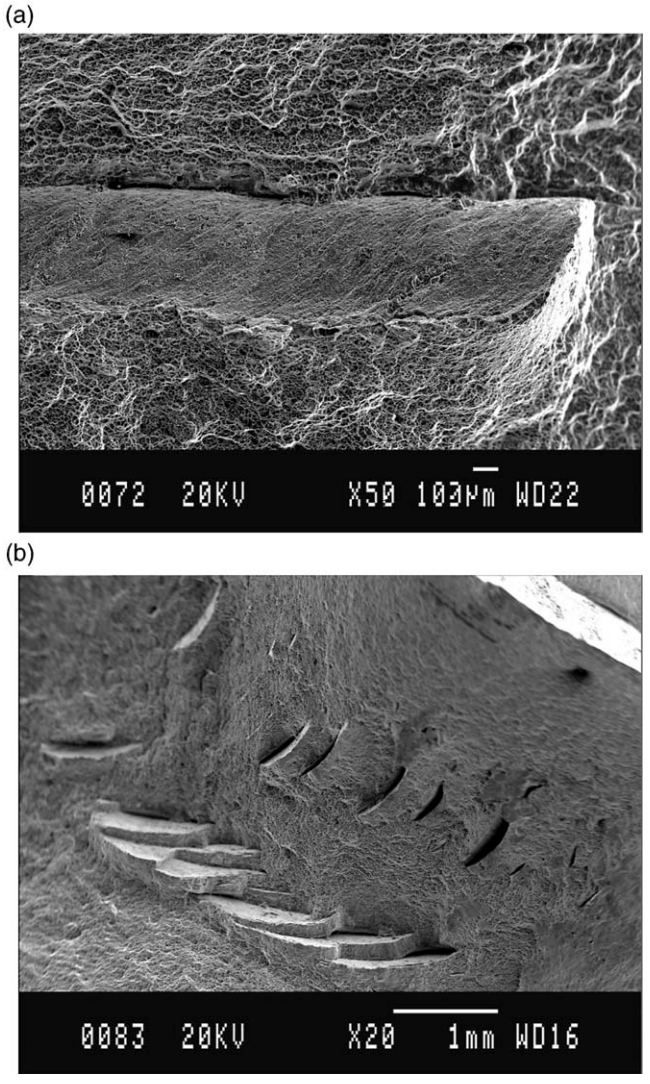

Fig. 10. (a) SEM fractograph showing a large partial-forging defect in specimen D10: N_f = 1,533,900 at $\sigma_{amplitude}$ = 80.4 MPa. (b) SEM fractograph of onion-skin defects in specimen D20: N_f = 1,551,600 at $\sigma_{amplitude}$ = 90.1 MPa.

in the fast fracture region. The onion-skin defects seen in specimen D10 (Fig. 10(b)) occur on the fast fracture region and hence had little effect on fatigue crack growth. Thus, the similar fatigue lives observed for two stress values that are some 12% different, appear to be primarily due to intrinsic variation in material properties. The forging-type defect in specimen D20 may, however, have reduced cyclic life in the crack growth region.

The influence of voids on crack initiation and of onion-skin forging defects in linking regions of fatigue cracks can be illustrated by considering fatigue data for two polished 95 mm/min specimens; B11: N_f = 565,000 at $\sigma_{amplitude}$ = 117.9 MPa and B5: N_f = 701,500 at $\sigma_{amplitude}$ = 140.0 MPa. The respective optical fractographs are shown in Fig. 11(a) and (b), and SEM fractographs are given in Fig. 12. Crack initiation in specimen B11 (Fig. 11(a)) can be seen to be linked to voids present near the surface (Fig. 12(a)), while in specimen B5, little evidence of such defects is present (Fig. 12(b)). Thus, a reduction in crack initiation life would be expected to have occurred. Additionally, as seen in Fig. 11(a), onion-skin defects in the fatigue region are present near the initiation site and will contribute to the reduction in the number of cycles representing crack growth to a critical size. In this case, the overall life of specimen B11 is reduced by a factor of 0.20, relative to specimen B5, at stress amplitude some 16% lower. This is a significant weld defect effect on fatigue life.

The effects of multiple crack initiation and crack linking via partial-forging defects can be illustrated via data for two polished 130 mm/min specimens; C9: N_f = 289,000 at $\sigma_{amplitude}$ = 125.0 MPa and C27: N_f = 246,700 at $\sigma_{amplitude}$ = 140.2 MPa. Optical fractographs of the two specimens are given in Fig. 13, and SEM fractographs of the crack initiation sites in the two specimens are provided in Figs. 14 and 15. It is clear that

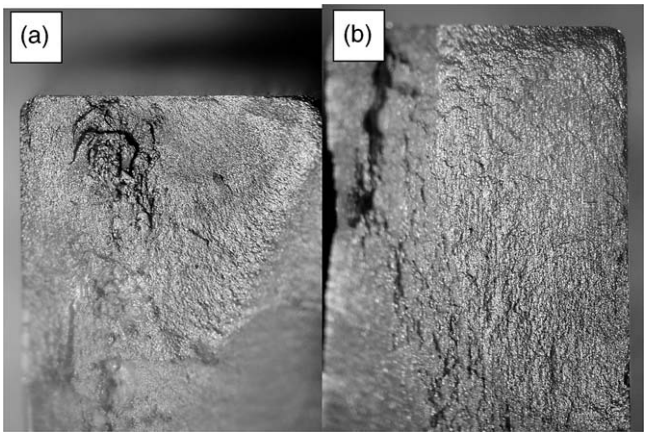

Fig. 11. Macroscopic fractographs showing two specimens welded at 95 mm/min: (a) Left—specimen B11: N_f = 565,000 at $\sigma_{amplitude}$ = 117.9 MPa; (b) right—specimen B5: N_f = 701,500 at $\sigma_{amplitude}$ = 140.0 MPa.

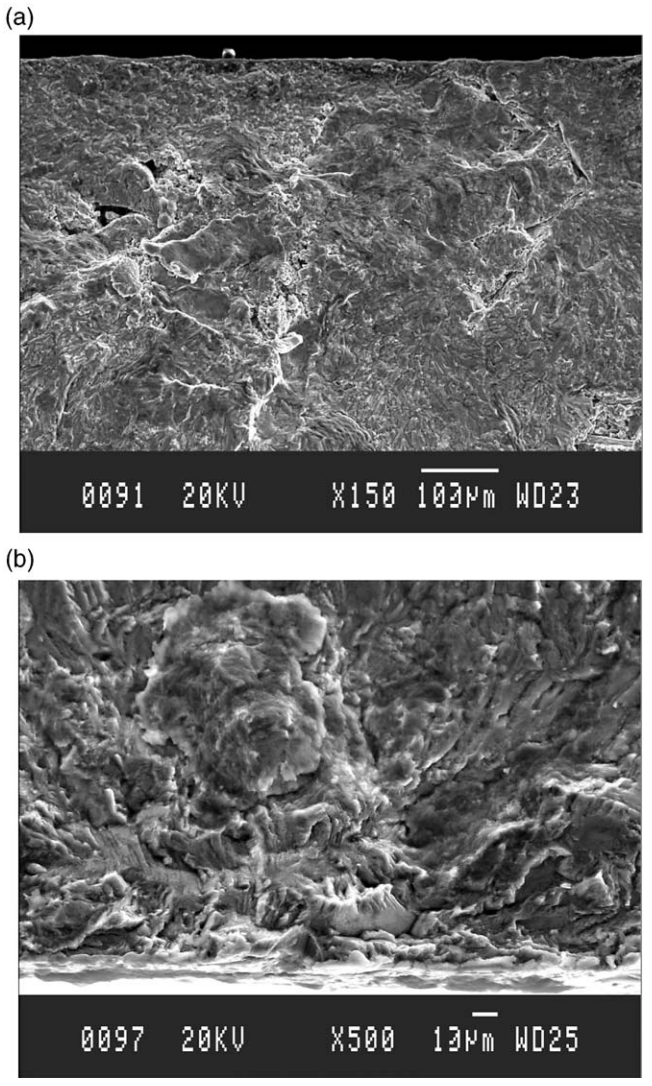

Fig. 12. (a) SEM fractograph showing the crack initiation region of specimen B11: N_f = 565,000 at $\sigma_{amplitude}$ = 117.9 MPa. (b) SEM fractograph showing the crack initiation region of specimen B5: N_f = 701,500 at $\sigma_{amplitude}$ = 140.0 MPa.

fatigue crack initiation is not associated with any specific defects, but that multiple cracks have initiated and joined along onion-skin defects (acting in a fashion analogous to tear ridges—Fig. 15). Interestingly, at this relatively high speed, the fatigue fracture surface detail shows more pronounced onion-skin texturing. Thus, weld microstructure is strongly reflected in the details of the fatigue crack growth, although its net influence is not easy to ascertain. This texturing effect is not as apparent on the fracture surface of specimens welded at 200 mm/min. It may therefore explain the slight drop in fatigue strength observed in the polished specimens welded at 130 mm/min, relative to the 200 mm/min samples. All as-welded specimens show crack initiation from surface tool marks in the weld region, and the reversed ranking of 130 and 200 mm/min specimens will

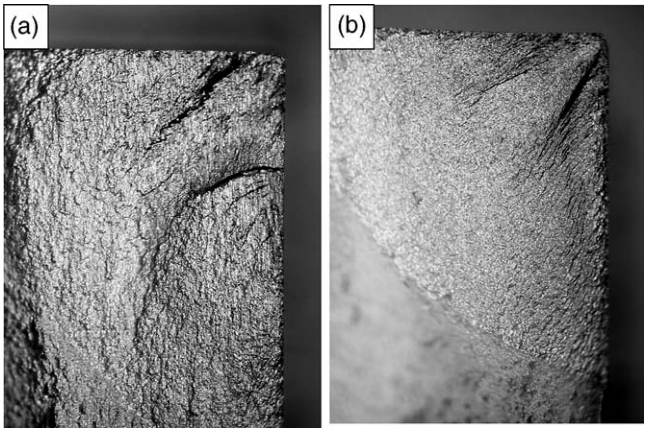

Fig. 13. Macroscopic fractographs showing two specimens welded at 130 mm/min: (a) Left—specimen C9: N_f = 289,000 at $\sigma_{amplitude}$ = 125.0 MPa; (b) right—specimen C27: N_f =246,700 at $\sigma_{amplitude}$ = 140.2 MPa.

then reflect the influence of parameters other than texture-induced enhanced early growth rates.

5. Conclusions

This study of influence of tool travel speed on the fatigue strength and occurrence of onion-skin partial-forging defects in single pass friction stir welds in 5083-H321 aluminium alloy has yielded the following conclusions.

1. Generally, there is a decrease in endurance limit stress (at 10^7 cycles) in both as-welded and polished specimens, as travel speed increases from 80 to 200 mm/min. The decrease has a maximum value of about 11% for polished and 19% for as-welded specimens. More in-depth metallography would be required to ascertain likely reasons for this.
2. The reversed ranking, relative to the 200 mm/min data, between polished and as-welded conditions at a travel speed of 130 mm/min is attributed to an influence of onion-skin texturing, which is reflected in the details of the fracture surface. This texturing appears to be more pronounced at this particular speed, than at other speeds, in these results.
3. Onion-skin forging-type defects (kissing bonds) occur with a similar frequency at all welding speeds, and hence do not appear to reflect the influence of a fluid dynamics vortex shedding mechanism.
4. Occasional voids are present in the welded specimens and these act as crack initiation sites if no larger defect is present at the surface. Overall life is then lowered relative to specimens where no voids are present.
5. Onion-skin defects are never associated with crack fatigue crack initiation, but occur at faster growth

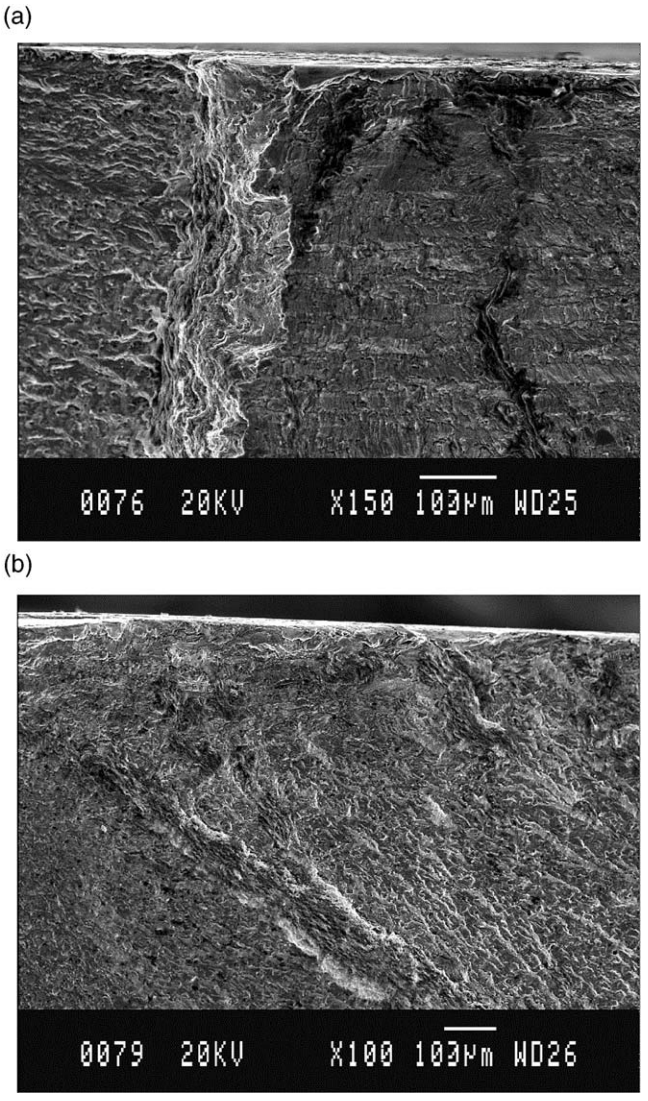

Fig. 14. (a) SEM fractograph showing the crack initiation region of specimen C9: N_f = 289,000 at $\sigma_{amplitude}$ =125.0 MPa. (b) SEM fractograph showing the crack initiation region of specimen C27: N_f = 246,700 at $\sigma_{amplitude}$ = 140.2 MPa.

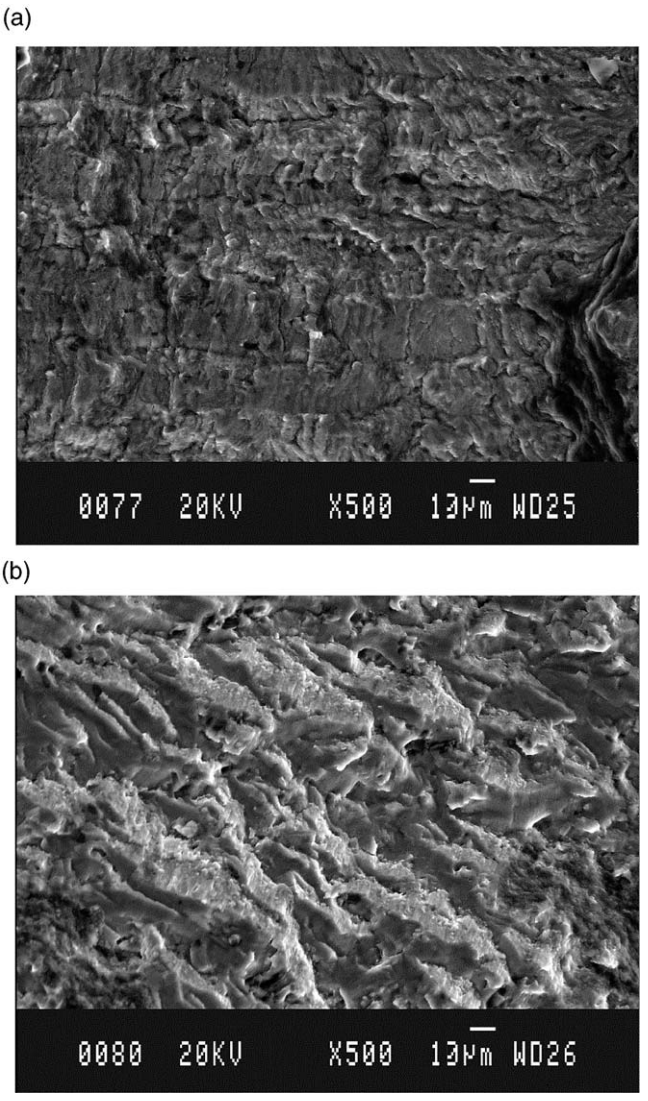

Fig. 15. (a) SEM fractograph showing the crack initiation region of specimen C9. Details of the onion-skin texture appear on the fractograph. (b) SEM fractograph showing the crack initiation region of specimen C27. Again, the onion-skin layers are apparent in the detail of the fracture surface.

rates, or in fast fracture. They can affect overall fatigue life, however, through providing easy linking paths between two initiated cracks. They may also have an effect on fracture toughness of FSW welds, and these aspects need attention.

Acknowledgements

This work was supported by Corus Research, Development and Technology, and the assistance of S. Webster and Dr T.J. Hurd is gratefully acknowledged. The assistance of TWI with the welding is also acknowledged.

References

[1] Webster PJ, Oosterkamp LD, Browne PA, Hughes DJ, Kang WP, Withers PJ, et al. Synchrotron X-ray residual strain scanning of a friction stir weld. Journal of Strain Analysis for Engineering Design 2001;36(1):61–70.
[2] Dalle Donne C, Biallas G, Ghidini T, Raimbeaux G. Effect of weld imperfections and residual stresses on the fatigue crack propagation in friction stir welded joints. In: Proceedings of the 2nd International Friction Stir Welding Symposium. Gothenburg, Sweden, June 2000. Abingdon: The Welding Institute; 2000.
[3] Lamarre A, Moles M. Ultrasound phased array inspection technology for the evaluation of friction stir welds. In: Proceedings of the 15th World Conference on Nondestructive Testing. Rome, Italy, October 2000. Brescia, Italy: Italian Society for Non-destructive Testing and Monitoring Diagnostics; 2000.
[4] Dickerson TL, Przydatek J. Fatigue of friction stir welds in alu-

minium alloys that contain root flaws. International Journal of Fatigue [doi: 10.1016/S0142-1123(03)00060-4].
[5] Ericsson M, Sandström R, Hagström J. Fatigue of friction stir welded AlMgSi-alloy 6082. In: Proceedings of the 2nd International Friction Stir Welding Symposium. Gothenburg, Sweden, June 2000. Abingdon: The Welding Institute; 2000.
[6] Bendzsak GJ, North TH, Smith CB. An experimentally validated 3D model for friction stir welding. In: Proceedings of the 2nd International Friction Stir Welding Symposium. Gothenburg, Sweden, June 2000. Abingdon: The Welding Institute; 2000.
[7] Ericsson M, Sandström R. Influence of welding speed on the fatigue of friction stir welds, and comparison with MIG and TIG. International Journal of Fatigue [doi: 10.1016/S0142-1123(03)00059-8].